Trends in Coastal Erosion by combining Satellite Image Analysis and Copernicus wave data: Paggaion Coastline, Northern Greece

K. Zachopoulos, N. Kokkos, M. Zoidou and G. Sylaios*

Laboratory of Ecological Engineering and Technology, Department of Environmental Engineering, Democritus University of Thrace, Vas. Sofias 12, 67100 Xanthi, Greece
Keywords: coastal processes; shoreline evolution; Satellite image classification; DSAS; GIS analysis.
*Corresponding author: gsylaios@env.duth.gr

Abstract

Coastal zones are facing intensified natural and anthropogenic disturbances including sea level rise, coastal erosion and over-exploitation of resources. Coastal zone monitoring of these effects involves satellite-borne shoreline extraction and detection of change rates over time. Shoreline changes are directly related to waves, tides, winds, storms, extreme events, sea level change and human activities affecting the geomorphologic processes of the coast. The shoreline evolution along the study site (Paggaion Municipality coastline, Northern Greece) was examined and assessed blending satellite-borne shoreline changes with the incident wave power, acting in the area during the latest decade (2009 - 2018). The study focuses on two geographical sub-areas: the eastern site representing the highly touristic sand dunes zone (Ammolofi), and the western site of Kariani-Orfani coastal zone, where significant erosion is evident. Both areas were selected based on their high economic and aesthetic values and the potential vulnerability to coastal erosion and climate changes impact, as identified by previous studies.

Keywords Coastal processes; Shoreline evolution; Satellite image classification; DSAS; GIS analysis.

1 INTRODUCTION

The coastal zone is a very dynamic geomorphologic system where changes occur at diverse temporal and spatial scales (Mills et al. 2005), mostly related to erosion, as a result of natural and/or anthropogenic activities (Van Rijn 2011). Natural effects include shoreline interactions with incident waves, tides, storms, tectonic and physical processes and the sediment load transported from the watershed by rivers (Dolan et al. 1980). Coastal zone monitoring is an important task for national/regional development and environmental protection, in which the assessment of the state of historic shorelines is important (Rasuly et al., 2010).

Coastal authorities are faced with the increasingly complex task of balancing development and managing coastal risks. Integrated Coastal Zone Management (ICZM) provides a framework to resolve conflicts, mitigate impacts of short-/long-term uses and support strategies for sustainable coastal management (Anfuso et al., 2011). The present study is focused on the dynamics of shoreline movement in Paggaion Municipality, Northern Greece. The area was selected based on its high economic, archaeologic and aesthetic values and the potential vulnerability to coastal erosion and their exposure to climate change impacts. The methodology carried out by examining and assessing the coastline erosion and accretion “hotspots” from the period 1986 to 2018, using lower and higher resolution historical satellite images. Furthermore, the incident wave power and wave angle acting in the coastal zone during the latest decade (2009 – 2018) was correlated to the erosion activity using higher resolution historical satellite images.

2 STUDY AREA

The study is focused on the southern shoreline of the Paggaion Municipality, Northern Greece (Figure 1). The total length of the shoreline is 36.3 km, covering the zone from Ofrinio to Ammolofi Beach. The study is focused on two geographical sub-areas: a) the eastern site, representing the highly-touristic sand dunes zone (Ammolofi), extending up to 50 m in width and approximately 20 km in length; and b) the western site of Orfani-Kariani coastal zone. Both areas have beach sediments composed of fine sand to very coarse sand (0.230 to 1.573 mm), separated by rocky peninsulas.

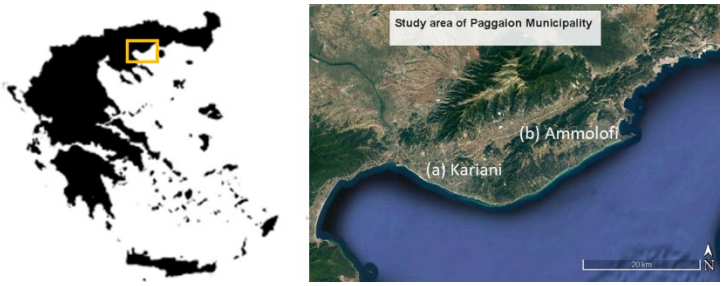

Figure 1 Study area of Paggaion Municipality (Kariani (a) and Ammolofi (b) study sites)

3 METHODOLOGY

3.1 Satellite Imagery

Eight historical satellite images were retrieved to cover the time period from 1986 to 2018 (Table 1). The historical image selection was mainly based on the correct geo-reference and on the image clarity from cloud cover. The monochromatic Near Infrared Band was selected for the image analysis and historic shoreline extraction.

The shoreline movement analysis was carried out into two different time periods, based on the spatial resolution of the examined satellite images: (a) satellite images from Landsat 4-5 TM during 1986 to 2009, with lower spatial resolution (pixel size of 30 m), retrieved from the Earth Explorer database of the United States Geological Survey Global Visualizer, and (b) satellite images from RapidEye and PlanetScope during 2009 to 2018, retrieved from Planet Explorer Beta, with higher spatial resolution of 5 m and 3.1 m, respectively.

Table 1 Data products and its specifications

Data Products	Resolution	Year of Image Acquisition	Source
Landsat 4-5 TM	30 m	20-04-1986 29-07-1999 08-04-2005 15-08-2009	Earth Explorer, USGS
RapidEye	5 m	23-06-2009 12-07-2012 18-07-2015	Planet Explorer Beta
PlanetScope	3.1 m	15-08-2018	

3.2 Coastline extraction from satellite images

The methodology employed in this study entailed the semi-automatic procedure of shoreline delineation, using a semi-automatic image classification technique. Historic satellite images were analyzed and their shorelines were extracted by applying the semi-automatic classification process, allowing the identification of materials in an image according to their spectral signature. For the classification process only the Near Infrared Band of the satellite images was used. The image was imported to Semi-Automatic Classification Plugin (SCP) for QGIS (Congedo, 2016) and we manually identified around 30 areas on each image by recognizing the two classes. The new raster file was classified by applying the minimum distance classification algorithm. The shoreline was extracted by vectorizing the classified raster image and applying a Gaussian filtering algorithm in order to smooth the polyline and receive a better fit to the coast.

3.3 Evaluation of the shoreline evolution

The shoreline analysis was performed in two time periods (1986 – 2009 and 2009 – 2018), based on the satellite image resolution. In order to evaluate the shoreline evolution, an analysis was carried out by the Digital Shoreline Analysis System (DSAS), provided by the USGS (Thieler et al., 2009). The DSAS procedure used transects positioned along the shoreline at distances of 20 m. The reference baseline required by the DSAS procedure was manually digitized and positioned offshore and parallel to the most recent shoreline (2018). A series of statistical indices was produced, such as the Net Shoreline Movement (NSM, meters) index, reporting the distance between the oldest and the earliest shorelines for each transect, the End Point Rate (EPR, m/y)

calculated by dividing the distance of Net Shoreline Movement by the time elapsed between the oldest and the most recent shoreline, and finally, the Weighted Linear Regression (WLR, m/y), in which the weight *w* is a function of the variance of the measurement uncertainty (Genz et al., 2007):

$$w = 1 / e^2 \quad (1)$$

where *e* is the shoreline uncertainty value. Using the data produced by the DSAS transects, a statistical analysis of the shoreline evolution along the study years was applied and various statistical parameters were calculated and analysed. The results were verified by applying two methodologies for outlier removal: the Interquartile Range (IQR) method and the method of extreme values removal (based on quantile distribution – 1%) to "clip" the data and remove the outliers. Both methods were applied in combination with an optical and empirical detection.

3.4 Wave Characteristics at the Breaker Zone and Incident Wave Energy Calculation

Historic offshore wave time-series data at fourteen data points, were retrieved from the reanalysis product of the Copernicus Marine Environmental Monitoring Service (CMEMS). Wave data were comprised of the daily time-series of the spectral significant wave height (H_{mo}), the zero up-crossing wave period (T_{o2}) and the wave direction relative to the north (ϕ_o). These data, as open sea significant wave height (H_o), wave period (T) and open sea direction (ϕ_o) were imported into a simple wave-ray model to transform the offshore wave characteristics into the wave characteristics at the breaker zone. More precisely, a long list of parameters was estimated such as; a) the wavelength [m], b) the wave celerity [m/s], c) the wave group celerity [m/s], d) the breaker zone, e) the significant wave height [m], f) the breaker was computed, g) the shoaling coefficient, h) the refraction coefficient, i) the wave dispersion coefficients at offshore and breaker zones, j) the wave direction at the breaker zone, k) the longshore wave-induced current, V_{long} [m/s], l) the incident wave energy at the breaker zone [J $m^{-1}s^{-1}$], m) the longshore sediment transport on annual basis [m^3 yr^{-1}]. All parameters were produced following the equations described by the Coastal Engineering Manual (2008). Therefore, the estimated longshore sediment transport at segments of the coastline, over selected periods, will be corelated to the assessed shoreline retreat/advancement rates.

4 RESULTS

4.1 Erosion and Accretion Hotspots

Investigation of the shoreline status from 1986 to 2018 reveals that severe erosion is noticed along the Paggaion Municipality coastline. The study was carried out in two steps: a) coarse shoreline analysis for the period 1986 to 2009, highlighting the erosion and accretion hotspots, and b) a more detailed investigation of shoreline change rates for the period 2009 to 2018, correlating the erosion results to the estimated incident wave power.

Table 2 Statistical parameters produced from DSAS for the two study areas; NSM (shoreline movement in m), WLR (erosion/accretion rate in m/y)

	Kariani 1986-2009		Ammolofi 1986-2009		Kariani 2009-2018		Ammolofi 2009-2018	
	NSM	WLR	NSM	WLR	NSM	WLR	NSM	WLR
Maximum accretion	34.37	1.33	26.90	1.37	97.72	10.83	21.06	2.27
Maximum erosion	-35.08	-1.47	-22.10	-1.03	-48.40	-5.37	-22.07	-2.28
Average erosion	-0.70	0.15	2.21	-0.10	-4.11	-0.53	-2.46	-0.25

The western coastal area covers the shoreline from Ofrinio to Kariani Beach. Several hotspots of erosion and accretion are observed along the western coastal zone for the time period 1986-2009, with average erosion rate of -0.10 m/y. High erosion rates are observed in the southern-east area of Kariani coastline (about -0.70 m/y) and in the zone located on the west side of the new port of Kariani (up to -1.47 m/y). On the other hand, the higher accretion rates are observed in the east side adjusted to the harbor with maximum shoreline movement of +34.37 m and accretion rate of +1.33 m/y. The eastern coastline of the study area covers the coastal zone from Loutra Eleftheron to Ammolofi Beach. The erosion activity in that area is significantly lower compared to the western coastal zone. More precisely, the average rate of total shoreline change is around -0.10 m/y, with maximum erosion rate of -1.03 m/y and maximum accretion rate of +1.37 m/y. The higher accretion rates are observed at the north-eastern site of Mirtofito beach, with maximum shoreline movement of +26.90 m

from 1986 to 2009. On the contrary, the higher shoreline retreatment of -22.10 m is observed at the western region of Eleochori Beach.

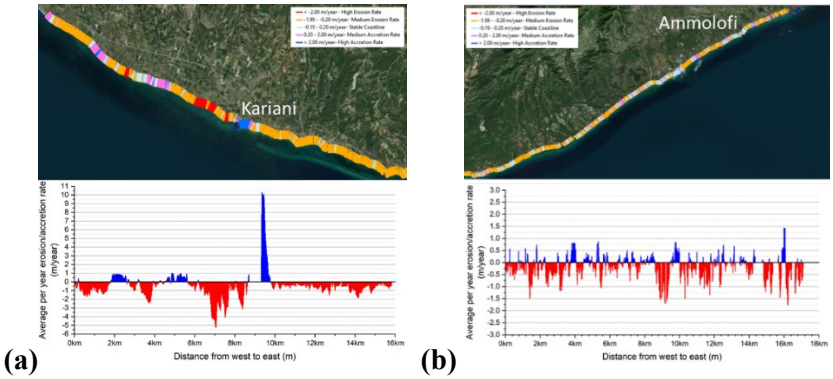

Figure 2 Erosion and accretion rate (WLR) in (a) Kariani and (b) Ammolofi study areas for the time period 2009 to 2018

Additionally, a more detailed study of evaluating the shoreline movement at both study areas was carried out for the time period 2009 to 2018, using higher resolution satellite images. In Kariani study site, the average shoreline retreat of -4.11 m is estimated, corresponding to an average erosion rate of -0.75 m/y. The higher shoreline erosion is observed at the west of the Kariani Port, with maximum erosion rate -5.37 m/y and coastal retreat of -48.40 m. In Ammolofi study site the average erosion rate is significant lower (-0.25 m/y). The higher erosion rates occurred mostly at the western sandy beaches of this area (-1.70 m/y) and at the central sector of Mirtofito beach (-1.62 m/y) (Figure 2b).

4.2 Correlation between Copernicus wave data and the erosion trends from 2009 to 2018

The incident wave energy prevailing over the study area influences sediment budget according to wave height and wave direction, which determine accretion or erosion features. More precisely, the mean incident wave energy in Kariani (239.93 J $m^{-1}s^{-1}$) is significantly higher than the wave energy in Ammolofi study site (102.32 J $m^{-1}s^{-1}$). The period 2009 to 2012 was the most energetic period with average wave power of 251.07 J $m^{-1}s^{-1}$ in Kariani and 109.98 J $m^{-1}s^{-1}$ in Ammolofi Beach. In both areas, shoreline retreat of -2.97 m and -2.56 m is observed. Moreover, for both study areas, the time period where the lower wave energy occurs corresponds to the period that slight shoreline accretion is observed.

In Kariani the most frequent incident wave orientation is ESE and SE with wave heights up to 3.6 m and the mean incident wave energy is estimated ~239.93 J $m^{-1}s^{-1}$. In that area the higher wave activity is observed in the south-eastern edge of Kariani shoreline, with estimated average incident wave energy of 260.24 J $m^{-1}s^{-1}$. At this beach segment the most significant shoreline movement of -2.10 m is observed in the same time period. Moreover, in Kariani the wave power and direction seem to affect the sediment transportation, moving from the south-eastern sandy beaches to the north-western coastal zone, thus confirming the DSAS results (Figure 2a).

On the other hand, in the Ammolofi study area, the wave power appears significantly lower (102.32 J $m^{-1}s^{-1}$) and the wave orientation is mostly from SSE and SE directions with wave heights up to 3.8 m. The wave crests reach the breaker zone at directions almost perpendicular to the shoreline, favoring cross-shore transport and the development of an extended sandy bar lowering the impact of erosion (-0.96 m). The higher erosion is observed at the eastern edge of Ammolofi beach, where the average incident wave energy is around 55 J $m^{-1}s^{-1}$ and the shoreline movement is approximately -1.20 m. The sandy dunes of Ammolofi are vulnerable to coastal erosion although lower wave activity occurs (Figure 2b).

The coastal erosion recorded from 2009 to 2018 is correlated to the incident wave energy on the coast and to the size of the sediment. Sandy beaches with fine grain sediment are more vulnerable to coastal erosion under the impact of high wave power. Moreover, the incident wave angle affects the wave power required to sediment flushing from the beach and also to the sediment transportation. In Kariani the average incident wave angle is around 118 degrees and the waves propagate from ESE to SE directions. In Kariani higher wave energy is required to transport the sediments from the south east to the north west of the study area. In contrast, in Ammolofi beach the wave direction is almost perpendicular to the shoreline (around 162 degrees) and the

waves propagate from SE to SSE directions. Although the erosion rates are relatively high, the wave power is significantly lower compared to Kariani.

Table 3 Parameters contributing to shoreline change at four indicative areas

Study Site	CMEMS points	Shoreline change (m)			Wave energy ($Jm^{-1}s^{-1}$)			Grain size (mm)		Wave angle (degrees)			Wave Orientation
		2009-2012	2012-2015	2015-2018	2009-2012	2012-2015	2015-2018			2009-2012	2012-2015	2015-2018	
Kariani	**182239**	-1.49	-1.64	1.55	295.81	276.45	250.71	0.485	Medium sand	118.11	118.21	118.98	ESE - SE
	182240	-2.40	-1.28	1.05	305.60	288.81	263.58	0.488	Medium sand	117.54	117.95	117.50	ESE - SE
Ammolofi	**183437**	-2.52	3.45	-3.74	74.29	60.79	72.16	0.230	Fine sand	160.76	161.71	155.65	SE - SSE
	183438	-3.01	2.58	-3.07	60.38	45.25	58.91	0.414	Medium sand	161.28	162.41	156.17	SE - SSE

5 CONCLUSION

The assessment of shoreline change using satellite images reveals that the study area has experienced high rates of erosion and accretion along the coastline during 1986 – 2018. Processes of erosion increased due to anthropogenic activities and natural conditions, such as wind and wave action. The erosion in the study area is affected both from the incident wave energy, the direction of waves propagation and the sediment grain size. The higher erosion rates correspond to periods of increased incident wave energy from directions favoring the longshore sediment transport. On the other hand, the lowest erosion rates correspond to segments that the coastline presents a smoother profile with minor changes in orientation. The present study constitutes a successful effort to correlate the offshore wave data given from the Copernicus Marine Environmental system to coastal erosion rates produced by historic satellite images.

Acknowledgement

This work was funded by the European Union and national funds of the participating countries in the framework of the INTERREG Balkan-Mediterranean Program, Project HERMES: "A HarmonizEd fRamework to Mitigate coastal EroSion promoting ICZM protocol implementation", Subsidy Contract BMP1/2.2/2546/2017.

References

Anfuso, G., Pranzini, E., & Vitale, G. (2011). An integrated approach to coastal erosion problems in northern Tuscany (Italy): Littoral morphological evolution and cell distribution. Geomorphology, 129(3-4), 204-214.

Congedo, L. (2016). Semi-automatic classification plugin documentation. Release, 4(0.1), 29.

Dolan, R.O.B.E.R.T., Hayden, B. P., May, P., & May, S. (1980). The reliability of shoreline change measurements from aerial photographs. Shore and beach, 48(4), 22-29.

Mills, J. P., Buckley, S. J., Mitchell, H. L., Clarke, P. J., & Edwards, S. J. (2005). A geomatics data integration technique for coastal change monitoring. Earth Surface Processes and Landforms: The Journal of the British Geomorphological Research Group, 30(6), 651-664.

Rasuly, A., Naghdifar, R., & Rasoli, M. (2010). Monitoring of Caspian Sea coastline changes using object-oriented techniques. Procedia Environmental Sciences, 2, 416-426.

Thieler, E. R., Himmelstoss, E. A., Zichichi, J. L., & Ergul, A. (2009). The Digital Shoreline Analysis System (DSAS) version 4.0-an ArcGIS extension for calculating shoreline change (No. 2008-1278). US Geological Survey

United States. (2008). Coastal engineering manual. Washington, D.C.: U.S. Army Corps of Engineers.

Van Rijn, L. C. (2011). Coastal erosion and control. Ocean & Coastal Management, 54(12), 867-88.